SuperMatching: Feature Matching using Supersymmetric Geometric Constraints
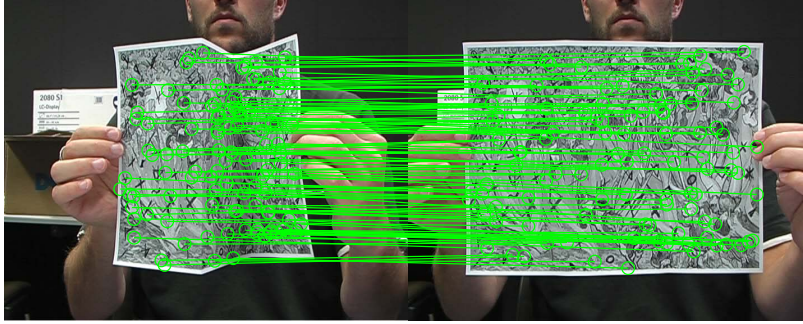

Figure 1: *Correspondences between 3D datasets determined by SuperMatching, using combined SIFT features (for color) and slippage features (for geometry). Left: rigid pairwise matching of views of a colored jug. Right: matching of a unfolded piece of paper with a large deformation.*

1 Abstract

Feature matching is a challenging problem lying at the heart of numerous computer graphics and computer vision applications. We present here the *SuperMatching* feature matching algorithm for finding correspondences between two sets of features. SuperMatching finds matches between feature points by considering triangles or higher-order tuples of points, going beyond the pointwise and pairwise approaches typically used. SuperMatching is formulated using a supersymmetric tensor representing an affinity metric which takes into account geometric constraints between features, since feature matching is casted as a higher-order graph matching problem. SuperMatching takes advantage of supersymmetry to devise an efficient sampling strategy to estimate the affinity tensor, as well as to store the tensor compactly. Matching is performed by computing a rank-one approximation of the tensor directly using a higher-order power iteration solution. Experiments on both synthetic and real captured data show that SuperMatching provides accurate feature matching for a wide range of 2D and 3D features, giving more reliable results than other state-of-the-art approaches, with competitive computational cost.

Keywords: Feature matching; Geometric constraints; Supersymmetric tensor

1 Introduction

Building correspondences between two sets of features belonging to a pair of 2D or 3D shapes is a fundamental problem in many computer graphics, geometry processing, and computer vision tasks. It arises in applications such as registration of partial or entire 3D shapes [Gelfand et al. 2005; Aiger et al. 2008; Li et al. 2008; Chang and Zwicker 2009; Zeng et al. 2010; van Kaick et al. 2011; Chang and Zwicker 2011], shape retrieval from databases [Bronstein et al. 2011], shape matching [Berg et al. 2005; Brown and Rusinkiewicz 2007; Torresani et al. 2008; Tevs et al. 2009; Ovsjanikov et al. 2010; Tevs et al. 2011; Sahillioglu and Yemez 2011; Windheuser et al. 2011], shape reconstruction [Brown and Rusinkiewicz 2007; Pekelny and Gotsman 2008; Wand et al. 2009; Chang and Zwicker 2011], and automatic shape understanding [Lipman and Funkhouser 2009; Sun et al. 2010; Kim et al. 2011] .

In principle and practise, determining correspondences is typically done in three steps [Johnson and Hebert 1999; Lowe 2004; Sun et al. 2009; Bokeloh et al. 2008; Toler-Franklin et al. 2010; Leutenegger et al. 2011]: (i) computing high-quality descriptors which serve to distinguish points from one another, (ii) choosing certain salient points with unusual feature descriptors, for matching, and (iii) determining the most suitable matching between the two sets of points. The former two problems have widely attracted considerable attention as their importance is easy perceivable. However, even supposing ideal feature descriptors and selectors that capture the most important and distinctive information about the neighborhood of each salient point, state-of-the-art algorithms still find it challenging to determine the best matching [van Kaick et al. 2011]. The reasons are various: real input data is noisy, and data may only be approximately in correspondence; the problem is further complicated by the presence of symmetric and congruent regions. Various feature matching algorithms have been devised to be robust in the presence of such issues. RANSAC-like algorithms [Tevs et al. 2009; Tevs et al. 2011] minimize the effects of outliers, generalized multidimensional scaling [Bronstein et al. 2011] and heat kernel maps [Ovsjanikov et al. 2010] consider the manifold in which the points are embedded. Möbius transformations [Lipman and Funkhouser 2009; Kim et al. 2011] also provide a powerful approach. However, these previous algorithms still do not treat the matching step as an independent problem, even if matching is not tightly coupled with feature description and selection. This paper focuses on the feature matching problem as a problem in its own right.

Matching may be done pointwise (single points to single points), or using tuples of points, for example point pairs separated by a fixed distance to other point pairs, triples of points forming a triangle to other triples of points, and so on. As pointed by [Conte et al. 2004], matching single features leads to a linear assignment problem, but if multiple features are matched at once, a quadratic or higher-order assignment problem results. Matching two feature sets by considering similarities of *single* features from each set can easily fail in the presence of ambiguities such as repeated elements, or similar local appearance. Quadratic and higher-order assignment matches groups of features, enforcing other constraints such as consistency of the distances between the points in each tuple being matched. This helps to reject many false matches, making the results more reliable in terms of greatly improving the matching accuracy. In general, feature similarity and satisfaction of constraints are expressed in terms of an affinity tensor relating pairs of point tuples.

As a particular example of *quadratic* assignment, Leordanu and Hebert [Leordeanu and Hebert 2005] consider pairs of feature descriptors, and use distances between pairs of features from each set to reduce the number of incorrect correspondences. Such pairwise distance constraints are particularly helpful in cases when the features themselves have low discriminative ability. The idea has been widely adopted in 3D shape matching algorithms [Tevs et al. 2009; Ovsjanikov et al. 2010; Tevs et al. 2011; Kim et al. 2011; Sahillioglu and Yemez 2011; Windheuser et al. 2011].

Higher-order assignment further generalizes the assignment problem to include yet more complex constraints between features. For example, third-order potential functions, used in [Duchenne et al. 2009; Zeng et al. 2010; Chertok and Keller 2010], quantify the affinity between two point triples by measuring the similarity of the angles of the triangles generated by such triples. However, this angular similarity value only considers the *total* difference in corresponding angles, and does not change with reordering of elements in the tuple. When similarity is expressed in this way, the affinity tensor becomes a *supersymmetric* tensor [Kofidis and Regalia 2002].

Our *SuperMatching* algorithm also formulates higher-order matching problems using a supersymmetric affinity tensor. It can accurately match a moderate number of features using triples or greater tuples of features. The contributions of this paper include:

- We show how to define a compact higher-order supersymmetric affinity tensor to express geometric consistent constraints between feature tuples.

- We make full use of the supersymmetry of the affinity tensor to devise a power iteration method to efficiently solve the matching problem.

- Complete computation of the full affinity tensor is computationally infeasible. We efficiently estimate it using a sampling strategy which takes advantage of supersymmetry. This avoids sampling repetitive items, it allows the tensor to be stored compactly, and also improves the matching accuracy by avoiding imbalances in sampling.

Our experiments using both synthetic and real captured data sets show that SuperMatching is more accurate and robust than prior methods, while having a similar computational cost. Importantly, the matching approach is general as it is independent of choice of 2D or 3D feature descriptors, feature point selection method, and constraints placed on tuples.

2 Related work

According to the applied constraints, previous approaches to feature matching can be classified into those which match single points to single points, those which match pairs of points to pairs of points, and so on.

Matching single points to single points is a linear assignment problem which only considers an affinity measure between two graph nodes, one from each set being matched; this measure is typically the feature distance between the two feature points. Affinity measures used in computer vision and computer graphics tasks rely heavily on descriptors computed using local information around each feature point, e.g. SIFT [Lowe 2004], spin images [Johnson and Hebert 1999], slippage features [Bokeloh et al. 2008], heat diffusion signatures [Sun et al. 2009], and BRISK [Leutenegger et al. 2011]. It is apparent that point-to-point matching is weak in that wrong correspondences maybe readily be established.

Matching pairs of points in one set to pairs of points in the other set leads to a quadratic assignment problem. The usual approach is now to take into account both similarity of the point features *and* the Euclidean/Geodesic distance between the points in a pair, assuming the objects are related by a rigid transformation [Leordeanu and Hebert 2005; Cour et al. 2006], or at least an isometry [Li et al. 2008; Tevs et al. 2009; Ovsjanikov et al. 2010; Tevs et al. 2011; Sahillioglu and Yemez 2011; Windheuser et al. 2011]. The quadratic assignment problem seeks to find a mapping which represents the optimal assignment. Unfortunately, this problem is NP-hard, unreasonable matching results could not be avoided.

Several higher-order approaches have also been proposed. Such higher-order methods can significantly improve matching accuracy, but higher-order assignment problem is more chanllenging, and various approximate methods have again been developed. Zass and Sashua [Zass and Shashua 2008] consider a probabilistic model of soft hypergraph matching. They reduce the higher-order problem to a first-order one by marginalizing the higher-order tensor to a one dimensional probability vector. Duchenne et al. [Duchenne et al. 2009] introduced a third-order tensor in place of an affinity matrix to represent affinities of feature triples, and higher-order power iteration was used to achieve the final matching. Chertok et al. [Chertok and Keller 2010] treat the tensor as a joint probability of assignments, marginalize the affinity tensor to a matrix, and find optimal soft assignments by eigendecomposition of the matrix. Wang et al. [Wang et al. 2010] also build a third-order affinity tensor, and obtain a final matching by rank-one approximation of the tensor. Higher-order assignment problems typically require large amounts of memory and computational resources. By reducing the number of elements needed to represent the affinity measures, the above approaches can match moderate numbers (many hundreds or more) of features. However, these 2D approaches still did not use the advantage of supersymmetric tensor, leading to a reduction in matching accuracy. For the harder 3D applications, there exits so many unpredictable issues.

A related idea using higher constraints in 3D registration, 4-points congruent sets method (4PCS), was proposed by Aiger et al. [Aiger et al. 2008]. It is a fast alignment scheme for 3D point sets that uses widely separated points. However, the coplanar 4 points and rigid-transformation constraints are some strong, and limit its applicability. We solve both rigid and isometric shape matching problem by one more mathematical and formulated tensor-based algorithm.

3 Overview

Assume we are given two sets of feature points P and Q, with N_1 and N_2 points respectively. The matching between these two feature sets can be represented by an *assignment variable* $\mathbf{X}$. $\mathbf{X}$ is a matrix, whose size is $N_1 N_2$ and elements are 0 or 1. $X(p, q) = 1$ when point $p \in P$ matches point $q \in Q$ and $X(p, q) = 0$ otherwise. $\mathbf{X}$ can be row-wise vectorized to give an assignment vector $\boldsymbol{x} \in \{0, 1\}^N$ where $N = N_1 N_2$.

Solving the higher-order matching problem is equivalent to finding the optimal assignment vector $\boldsymbol{x}^* = <x_{i_1}, \cdots, x_{i_N}> \in \{0, 1\}^N$, satisfying

$$\boldsymbol{x}^* = \arg\max_{\boldsymbol{x}} \sum_{i_1, \cdots, i_N} \mathcal{T}_r(i_1, \cdots, i_N) x_{i_1} \cdots x_{i_N}. \quad (1)$$

Here, i_n stands for an assignment (p_n, q_n), $(p_n \in P, q_n \in Q)$, and the product $x_{i_1} \cdots x_{i_N}$ means the tuple of features $(p_1, \cdots, p_{N_1})$ from P is matched to the tuple of features $(q_1, \cdots, q_{N_2})$ from Q. $\mathcal{T}_r(i_1, \cdots, i_N)$ defines the affinity of the set of assignments $\{i_n\}_{n=1}^N$; it is the affinity measure between the ordered feature tuples $(p_1, \cdots, p_{N_1})$ and $(q_1, \cdots, q_{N_2})$. In the paper, *the affinity*

measures would be defined based on the geometric constraints between pairs of feature tuples, this is the basis of the SuperMatching algorithm.

In the rest of the paper, we consider the one-to-many correspondence problem. We assume that each point in P is matched to exactly one point in Q, but that the reverse is not necessarily true. If *do* we want to treat both datasets in the same way, we can first match P to Q, then match Q to P, and then combine the matching results by taking their union or intersection. Uniqueness of matches for P means that the assignment variable matrix $\mathbf{X}$ satisfies $\sum_p X(p, q) = 1$.

From Equ.(1) we can see that there are four issues to be considered when using higher-order matching algorithms. How should we:

- organize and express the affinity measures $\mathcal{T}_N$ in a storage efficient manner? (see Section 4.1)

- approximately solve the optimal higher-order assignment problem efficiently? (see Section 4.2)

- define the affinity measure between two feature tuples? (see Section 4.3)

- determine an appropriate sampling strategy to estimate the affinity tensor in a way which will give good matching accuracy? (see Section 4.4)

4 SuperMatching

We first discuss the former two issues mentioned above, which are independent of application; later we turn to definition of affinity measure, which is application dependent, and sampling strategy.

4.1 Supersymmetric Affinity Tensor

A tensor generalizes vectors and matrices to higher dimensions: a vector is a tensor of order one, and a matrix is a tensor of order two. A higher-order tensor can be expressed as a multi-dimensional array [Kolda and Bader 2009]. Here we consider a higher-order supersymmetric affinity tensor, which represents a real-valued higher-order affinity between feature tuples. The main motivation of using supersymmetry is try to utilize its advantage to remove the redundancy of the tensor elements, and the following deduction would prove that the motivation is effective.

Definition 1 (Supersymmetric Tensor) *A tensor is* supersymmetric *if its entries are invariant under any permutation of its indices [Kofidis and Regalia 2002].*

For example, a third-order supersymmetric tensor $\mathcal{T}_3$, satisfies the relationships: $\mathcal{T}_3(i_1, i_2, i_3) = \mathcal{T}_3(i_1, i_3, i_2) = \mathcal{T}_3(i_2, i_1, i_3) = \mathcal{T}_3(i_2, i_3, i_1) = \mathcal{T}_3(i_3, i_1, i_2) = \mathcal{T}_3(i_3, i_2, i_1)$.

Definition 2 (Supersymmetric Affinity Tensor) *Given two feature sets P and Q, with N_1 and N_2 features respectively, the supersymmetric affinity tensor is an rth order $I_1, \cdots, I_N$, nonnegative tensor $\mathcal{T}_r$, where $I_1, \cdots, I_N = N_1 N_2$, for which there exists a set of indices θ_N, and an rth order potential function ϕ_r, such that*

$$\mathcal{T}_r(i_1, \ldots, i_N) = \begin{cases} \phi_r(\Omega(i_1, \ldots, i_N)) & , \forall(i_1, \ldots, i_N) \in \theta_N \\ 0 & , \forall(i_1, \ldots, i_N) \notin \theta_N \end{cases}$$
(2)

where Ω stands for an arbitrary permutation of the vector, and θ_N satisfies $\forall(i_1, \ldots, i_N) \in \theta_N, \forall i_m \in \{i_1, \ldots, i_N\}$ and $\forall i_n \in \{i_1, \ldots, i_N\} - \{i_m\}$ meets the requirement that $i_m \neq i_n$.

Algorithm 1 Higher-order power iteration method for a supersymmetric affinity tensor (with $\mathcal{C}_1$ norm)

Input: r^{th}-order supersymmetric affinity tensor elements
Output: unit-norm vector $\boldsymbol{u}$

1: Initialize $\boldsymbol{u}_0$ by randomly positive values, $k = 1$
2: **repeat**
3:    **for** all $(i_1, i_2, \cdots, i_N) \in \theta_N$ **do**
4:       **for** all $m \in (i_1, \cdots, i_N)$ **do**
5:          $v_m^{(k)} = (N-1)! \phi_r(i_1, \cdots, i_N) 2 v_m^{2(k-1)} v_{i_1}^{2(k-1)} \cdots$
                $v_{m-1}^{2(k-1)} v_{m+1}^{2(k-1)} \cdots v_{i_N}^{2(k-1)}$
6:       **end**
7:       **for** $i = 1 : N_1$ **do**
8:          $v^{(k)}(((i-1) \cdot N_2 + 1) : i \cdot N_2) =$
         $\hat{v}^{(k)}(((i-1) \cdot N_2 + 1) : i \cdot N_2)/\|\hat{v}^{(k)}(((i-1) \cdot N_2 + 1) : i \cdot N_2)\|_1$
9:       **end**
10:    **end**
11:    $k = k + 1$;
12: **until** convergence;
   Note: $\boldsymbol{u}^{(k)} = \boldsymbol{v}^{2(k)}$, ϕ_N is the corresponding potential function, and $v^{(k)}(((i-1) \cdot N_2 + 1) : i \cdot N_2)$ denotes the slice of $v^{(k)}$ with indices from $(i-1) \cdot N_2 + 1$ to $i \cdot N_2$.

A tensor element with $(i_1, \ldots, i_N) \in \theta_N$ is called as a *potential element*, while other elements are called *non-potential element*. The potential element is one final matching result from all possible matching candidates.

Using Definition 2, we now can greatly reduce the amount of storage needed, representing every potential element $\mathcal{T}_r(i_1, \ldots, i_N)$ by the canonical entry $\mathcal{T}_r(\text{sort}(i_1, \ldots, i_N)), \forall(i_1, \ldots, i_N) \in \theta_N$. Each stored value thus provides the value for $N!$ entries. As non-potential elements all have value zero, there is no need to store them. This greatly reduces both storage, and sampling needed for feature tuples when estimating the affinity tensor, as discussed in Section 4.4. At the same time, it can be used to make the power iteration process more efficient: see Section 4.2.

4.2 Higher-order Power Iteration Solving

Using Definition 2, Equ.(1) can be expressed as:

$$\boldsymbol{x}^* = \arg\max_{\boldsymbol{x}} \sum_{i_1, i_2, \cdots, i_N} \mathcal{T}_r(i_1, \cdots, i_N) x_{i_1} \cdots x_{i_N}$$
$$= \max <\mathcal{T}_r, \boldsymbol{x}^{\star N}>$$
(3)

where $\star$ is called the Tucker product [Kofidis and Regalia 2002], and $\boldsymbol{x} \in \{0, 1\}^N$. Solving Equ.(3) is an NP-complete problem, so it is common to relax the constraints: the binary assignment vector $\boldsymbol{x} \in \{0, 1\}^N$ is replaced by an assignment vector $\boldsymbol{u}$ with elements taking real values in $[0, 1]$. This changes the optimization problem to one of computing the rank-one approximation of the affinity tensor $\mathcal{T}_r$ [Kofidis and Regalia 2002], i.e. finding a scalar λ and a unit norm vector $\boldsymbol{u} \in \mathbb{R}^N$, such that the tensor $\hat{\mathcal{T}}_r = \lambda \boldsymbol{u} \star \boldsymbol{u} \star \cdots \star \boldsymbol{u} = \boldsymbol{u}^{\star N}$ minimizes the function $f(\hat{\mathcal{T}}_r) = \|\mathcal{T}_r - \hat{\mathcal{T}}_r\|$. The final matching result is found by replacing each element of $\boldsymbol{u}$ by 0 or 1 according to whichever it is closer to.

The higher-order power method is commonly used to find the rank-one tensor approximation; a version for supersymmetric tensors (S-HOPM) is given in [Kofidis and Regalia 2002]. The S-HOPM algorithm converges under the assumption of convexity for the functional induced by the tensor [Kofidis and Regalia 2002], which is sufficiently robust for practical application. S-HOPM is performed in two iterative steps: higher-order power iteration of $\boldsymbol{u}$, followed

by normalization of $\boldsymbol{u}$ under the Frobenius norm. A recent effective improvement [Duchenne et al. 2009] uses the $\mathcal{C}_1$ norm to replace the traditional $\mathcal{C}_2$ norm.

We both use the $\mathcal{C}_1$ norm, and further revise S-HOPM as follows. To perform higher-order power iteration of $\boldsymbol{u}$, we must compute $\hat{\boldsymbol{u}}^{(k)} = \mathcal{I} \overset{\mathcal{T}_r}{\star} (\boldsymbol{u}^{(k-1)})^{\overset{\mathcal{T}_r}{\star}(N-1)}$, where $\overset{\mathcal{T}_r}{\star}$ is a so-called $\mathcal{T}_r$-product, and $\mathcal{I}$ is the unit tensor [Kofidis and Regalia 2002]. For $\hat{\boldsymbol{u}}^{(k)}$ belonging to an rth-order supersymmetric affinity tensor, this can be formulated as follows:

$$\hat{\boldsymbol{u}}^{(k)} = \mathcal{I} \overset{\mathcal{T}_r}{\star} (\boldsymbol{u}^{(k-1)})^{\overset{\mathcal{T}_r}{\star}(N-1)} \text{ implies that } \forall m \in (i_1, ..., i_N),$$
$$v_m^{(k)} =$$
$$\sum_{i_1,...,i_N} \mathcal{T}_r(i_1, ..., i_N) 2 v_m^{(k-1)} v_{i_1}^{2(k-1)} ... v_{m-1}^{2(k-1)} v_{m+1}^{2(k-1)} ... v_{i_N}^{2(k-1)} =$$
$$(N-1)! \phi_r(i_1, ..., i_N) 2 v_m^{(k-1)} v_{i_1}^{2(k-1)} ... v_{m-1}^{2(k-1)} v_{m+1}^{2(k-1)} ... v_{i_N}^{2(k-1)} \tag{4}$$

where $\boldsymbol{u}^{(k)} = \boldsymbol{v}^{2(k)}$, and ϕ_r is corresponding potential function that would be detailed in the following Section 4.3. Our revised S-HOPM relies on two principles. First, we take advantage of the supersymmetry to deduce $\boldsymbol{u}$ as Equ.(4). Secondly, many of the elements of the affinity tensor are zero non-potential elements: it is much more efficient to perform the power iteration by just considering the non-zero potential elements.

Our supersymmetric higher-order power iteration solution is summarised in Algorithm 1. It excludes each non-potential element from the iteration process, so it is efficient. And the complexity of the whole iteration process only depends on the number $|\theta_N|$ of non-zero affinities. Step 5 in Algorithm 1 represents all permutations of each potential element $\mathcal{T}_r(i_1, \cdots, i_N)$ using a single potential function $\phi_r(i_1, \cdots, i_N)$. Consequently, this method reduces memory costs while keeping accuracy. Note that, although [Duchenne et al. 2009] claimed to use a supersymmetric affinity tensor, this approach does not make full use of supersymmetry when creating the supersymmetric affinity tensor, nor does it take advantage of supersymmetry to accelerate the power iteration process. By doing so, we overcome limitations due to unbalanced and redundant tensor elements in [Duchenne et al. 2009], as our experiments show later.

Many initialization schemes have been proposed for the S-HOPM method [Kofidis and Regalia 2002]. We simply use positive random values to initialize $\boldsymbol{u}_0$, which ensures convergence.

4.3 Higher-order Potentials

Different higher-order potentials are appropriate for different applications. Here we give two general higher-order potentials. One may be used for 2D cases, while the other is defined for 3D matching. The potentials are based on a Gaussian function which guarantees the tensor elements are non-negative and invariant to any permutation of the input assignments.

In 2D, we first restate a well-known 2D third-order geometric-similarity invariant potential ϕ_3 [Duchenne et al. 2009; Chertok and Keller 2010] for linking two point feature triples. Similarity of triangles formed by three points corresponds to invariance under scaling, rotation and translation—interior angles do not change. Thus ϕ_3 can be defined in terms of differences of corresponding interior angles:

$$\begin{aligned} \phi_3(i_1, i_2, i_3) &= \phi_3(\{p_1, q_1\}, \{p_2, q_2\}, \{p_3, q_3\}) \\ &= \exp(-1/\varepsilon^2 \sum_{(l,l')} \|\alpha_l - \alpha_{l'}\|^2) \end{aligned} \tag{5}$$
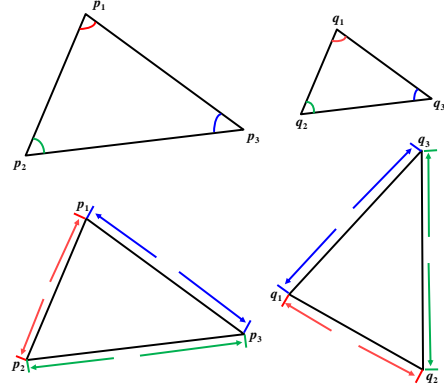

Figure 2: *Third-order potential. The geometric constraints are: internal angle invariance in 2D (above), and edge length invariance in 3D (below).*

where $\varepsilon > 0$ is the is the kernel bandwidth, $\{\alpha_l\}_{l=1}^3$ and $\{\alpha_l'\}_{l'=1'}^3$ are the angles formed by feature triples (p_1, p_2, p_3) and (q_1, q_2, q_3): see Figure 2. Each point corresponds to one interior angle. We may extend it to the general case by using the internal angles formed by higher degree polygons. It is easy to see that the potential preserves invariance under rigid transformations in 2D field.

For 3D matching problems, we may replace the internal angle by edge length, i.e., the geodesic distance across the mesh in which the points are embedded., which now corresponds an isometry transform relating the point sets. The geodesic distance is computed by the Dijkstra algorithm [Peyré et al. 2010] .

We will use these two high-order potentials to evaluate our algorithm. Figure 2 illustrates the schematic diagram of third-order potential in 2D and 3D cases.

4.4 Sampling strategy

Algorithm 1 depends on all potential elements. We next discuss the issue of how to sample the feature tuples to build potential items, which determines the size $|\theta_N|$ and influences matching accuracy.

For the two feature sets P and Q, a potential element may be obtained by using two feature tuples sampled from each feature set separately. For rth-order matching, a naive way to construct the potential elements is as follows: first find all feature tuples for P and Q, as F_1 and F_2; then $\forall(f_{i_1}^1, \cdots, f_{i_N}^1) \in F_1$, calculating the potentials for $(f_{i_1}^1, \cdots, f_{i_N}^1)$ with all feature tuples in F_2. This naive method is very time-consuming, which is why sampling is used. We employ random sampling for general feature matching problems, but this does not preclude more directed sampling if prior knowledge of the matching problems gives guidance.

Our sampling approach is to repeatedly randomly sample t_1 feature tuples from P, and fully sample Q to find all N_2^r feature tuples. For P, in order to cover all features in P as F_1, we repeatedly take one feature as a required element, and then randomly choose t_1 feature tuples containing this required element. We repeat this process until all features in P have been chosen once as a required element. Then, $\forall(f_{i_1}^1, \cdots, f_{i_N}^1) \in F_1$, we find r most similar features in F_2 to build r potential elements as ϕ_i^r. Combining all the potential elements obtained, we form the desired potential element set $\theta_N = \{\phi_i^r\}_{i=1}^{N_1 t_1}$, of size $|\theta_N| = N_1 t_1 r$. For P, the sampling cost is $O(N_1 t_1 r)$. The parameters t_1 and r must be chosen according to the size of the feature sets. In practice, for two feature sets each

with hundreds points, we may take $t_1 \approx 100$ and $r = 3$ for third-order matching. Our experiments demonstrate that this sampling approach works well.

The most important part of our sampling approach is to use the supersymmetry of the affinity tensor. Potential elements whose indices are permutations of each other have the same value, so should not be repeatedly sampled. Thus, we use a sampling constraint that the sets of feature tuples F_1 obtained from the sampling process should have no repetition, in the sense that

$$\forall (f_{i_1}^1, f_{i_2}^1, \cdots, f_{i_N}^1), (f_{j_1}^1, f_{j_2}^1, \cdots, f_{j_N}^1) \in F_1,$$
$$(f_{i_1}^1, f_{i_2}^1, \cdots, f_{i_N}^1) \neq \Omega(f_{j_1}^1, f_{j_2}^1, \cdots, f_{j_N}^1) \quad (6)$$

where Ω is an arbitrary permutation.

Earlier work [Duchenne et al. 2009; Zass and Shashua 2008] adopted random sampling, but failed to impose any constraint on the sampling process, leading to the possibility that feature tuples may be sampled multiple times. For example, for third-order matching, it is possible that a feature tuple $(f_{i_1}^1, f_{i_2}^1, f_{i_3}^1)$ may be sampled from P and $(f_{i_1}^2, f_{i_2}^2, f_{i_3}^2)$ from Q, and also a feature tuple $(f_{i_1}^1, f_{i_3}^1, f_{i_2}^1)$ sampled from P and $(f_{i_1}^2, f_{i_3}^2, f_{i_2}^2)$ from Q. That will create two tensor elements $\phi_3(s_{i_1}, s_{i_2}, s_{i_3})$ with index $(s_{i_1}, s_{i_2}, s_{i_3})$ and $\phi_3(s_{i_1}, s_{i_3}, s_{i_2})$ with index $(s_{i_1}, s_{i_3}, s_{i_2})$, which are the same. However, we just need one tensor element to express the affinity measure on the assignment group $(s_{i_1}, s_{i_2}, s_{i_3})$ for any permutation of indices. This extra sampling is not only inefficient, but may also reduce the accuracy of the power iteration: one set of symmetrically related elements may be represented by a different number of samples than another set of symmetrically related elements, which unbalances the power iteration process, and can lead to inaccurate results. Therefore, our sampling method reduces the sampling cost, while also improving the accuracy of the power iteration.

5 Experiments

We have used synthetically generated data as well as real captured data to evaluate the SuperMatching algorithm. To demonstrate that the SuperMatching algorithm is general (independent of feature descriptors), several descriptors have been used. For the input shapes without color information, slippage features [Bokeloh et al. 2008] were employed. For 3D coloured shapes, both SIFT and slippage features were used. We used third-order matching in our experiments, and note it would be simple to use higher order.

5.1 3D rigid shapes scans

Firstly, we used SuperMatching to pairwisely align 3D rigid shape scans. The rigid transforms can be computed from the three compatible matching feature points. The transform which brings the most data points within a threshold of a point in the model is chosen as the optimal aligning transform [Huttenlocher and Ullman 1990]. As discussed in [Gelfand et al. 2005], such a voting scheme is guaranteed to find the optimal alignment between the pairwise scans and is independent of the initial pose of the input scans. Figure 3 shows two registration examples of articulated model, the right is the failure case by [Aiger et al. 2008].

In the following, we extended the SuperMatching to build a complete model from a set of scans from different viewpoints. For the multiple scans, the third-order matching is first performed between two consecutive scans. After the initial pairwise matching, the alignment is refined by the iterative closest point (ICP) algorithm following [Gelfand et al. 2005]. Figure 4 illustrates the approach.
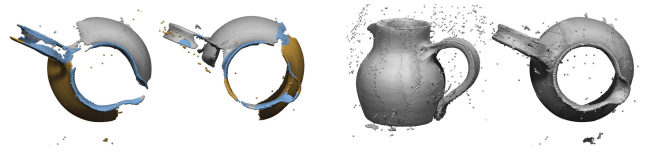

Figure 3: *Pairwise alignment of xx. The right is the result from [Aiger et al. 2008]. On the coming :)*

Above, a sheep's head is scanned from multiple viewpoints. Below, matching is used to align 10 scans which are then merged to produce a single shape. Pairs of consecutive scans, linked by dark segments, are matched using the SuperMatching algorithm.
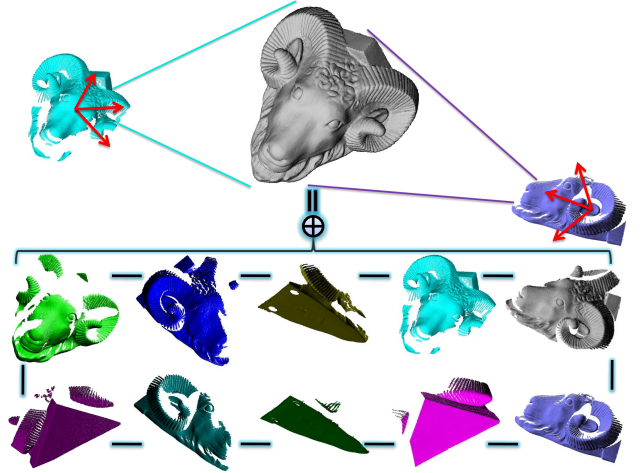

Figure 4: *Alignment of several sheep head scans from different viewpoints. Above: scans are captured from different viewpoints. Below: the final shape is formed from 10 aligned scans, the dark segments imply where the pairwise matching works.*

5.2 3D depth scans with color information

Complementary to the evaluation presented above, we also provide a real-world noisy example demonstration of SuperMatching. In this case, real world data with surface color information was captured using a Kinect camera [Kinect 2012], and both SIFT and slippage features were used as a basis for SuperMatching, which resulted in robust matches without significant outliers, as illustrated in Figure 5. The example also demonstrates that the SuperMatching is general, i.e., independent of feature descriptors.

5.3 3D articulated shape synthetic data

Thirdly, we present another application, registration of (approximately) articulated shapes. Such problems are common in dynamic range scanning. Given a sequence of range scans of a moving articulated subject, our method automatically registers all data to produce a complete 3D shape. Note that, unlike many other methods, our method does not need any of manual segmentation, user specified markers, or a prior template. While the problem of non-rigid registration of deformable shapes is ill-posed and no algorithm is applicable to all scenarios, we believe that our approach pushes the limits of what can be achieved with minimal prior information, and is robust to partial data with holes.

For the pairwise articulated shape registration, although the par-

Figure 5: *3D real depth scans with color information, captured using Kinect. Above: two given different local pre-scans. Below: a single scan. Matching points are connected by green lines.*

reconstruction over all frames as $0.001D$ where D is the bounding box diagonal length, and the greatest distance error in any one frame was $0.012D$.

Figure 7: *The registration of articulated hand. Above: partial synthetic data with holes is generated from a deformation sequence. The reconstructed meshes are deduced from the registration process (center). Below: ground truth shape, and average and maximum distance from the ground truth per frame.*

tial scans have missing data and their poses are different, Super-Matching still produces accurate matching. Correspondences between slippage feature points are established by SuperMatching; these permit robust registration of scans by computing piecewise rigid transformations. These transformations are propagated from the slippage feature points to the entire set of points in each scan using nearest neighbor interpolation. Figure 6 shows two registration examples of articulated model, the right is the failure case by [Chang and Zwicker 2009].
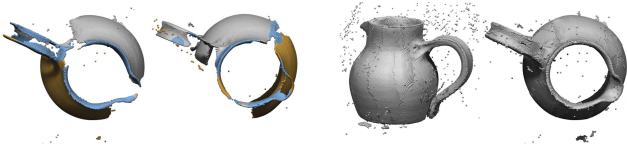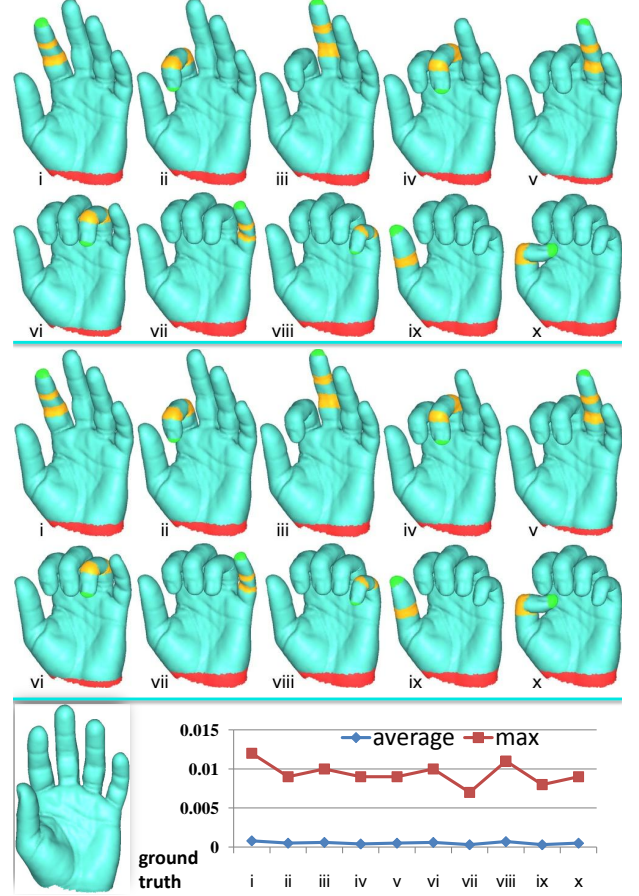

Figure 6: *Pairwise alignment of articulated xx. The right is the failure case by [Chang and Zwicker 2009]. On the coming :)*

For a sequence of partial articulated data, the registration is performed int two main steps. We first precompute an initial pairwise registration for each pair of consecutive frames, then perform articulated shape reconstruction as in [Pekelny and Gotsman 2008]. The pairwise registration is addressed as former paragraph. Segmentation of the scans into rigid parts can readily be done by clustering the transformations obtained from the slippage feature points, using the mean shift algorithm [Comaniciu and Meer 2002]. This information is used as the input to the second step of articulated shape reconstruction following [Pekelny and Gotsman 2008]; this algorithm identifies and tracks the rigid parts in each frame, while accumulating geometric information over time. However, [Pekelny and Gotsman 2008] requires the user to manually segment each range scan in advance, whereas we automatically determine the segmentation. Figure 7 shows an articulated hand example. This synthetic data is generated from a deformation sequence, and the final registered shape is produced from these partial data. By using synthetic data, we are able to evaluate the robustness of our reconstruction method using the ground truth, as shown below in Figure 7. Quantitatively, we measured the maximum of the average distance of the

5.4 Deformable surfaces

Finally, we matched SIFT points showing deforming surfaces[1]; these showed a cloth and a cushion. The surface of the cloth underwent relatively smooth deformations, while the surface of the cushion included sharp folds. This data comes with ground truth, which allows quantitative verification of the accuracy of the matches found. From each surface set we randomly chose two frames before and after a large deformation. We randomly chose 100 corresponding points on each surface to be the features, using the provided ground truth.

We used the above input data as a basis for comparison with the spectral algorithm [Cour et al. 2006] (a quadric assignment algorithm), a third-order tensor algorithm [Duchenne et al. 2009], and the hyper graph matching algorithm [Zass and Shashua 2008], using the authors' code in each case. All methods were executed in Matlab on a 2.3GHz Core2Duo with 2GB memory. To enable direct and fair comparison, [Duchenne et al. 2009], [Zass and Shashua

---

[1]From http://cvlab.epfl.ch/data/dsr/

2008] and SuperMatching used the same potential and all maintained an equivalent tensor size N.

In the tests, SuperMatching considered 30000 feature tuples, while the method of [Duchenne et al. 2009] considered 1010000 features and the method of [Zass and Shashua 2008] used 40000. The difference mainly results from differences in sampling strategy; note that we have the lowest sampling cost. The average running time to match two feature sets each with 100 features was around 8s for SuperMatching, 13s for [Duchenne et al. 2009], 6.5s for [Zass and Shashua 2008], and 5s for [Cour et al. 2006]. SuperMatching takes less than the third-order tensor algorithm in [Duchenne et al. 2009] as it uses the same tensor size but fewer feature tuples.

Matching accuracy is assessed as the number of correctly matched points (according to the provided ground truth) divided by the total number of points that could potentially be matched. The results are summarised in Table 1 and illustrated in Figure 8. Table 1 demonstrates that SuperMatching achieves a higher matching accuracy than previous algorithms. The worst matching result is produced by the spectral quadratic assignment algorithm [Cour et al. 2006], due to the lower discriminatory power of the pairwise geometric constraints used. Higher-order algorithms perform much better due to the more complex geometric constraints. Nevertheless, SupeMatching outperforms the third-order algorithm [Duchenne et al. 2009] and the hyper graph matching algorithm [Zass and Shashua 2008], as these do not tale proper advantage of supersymmetry.
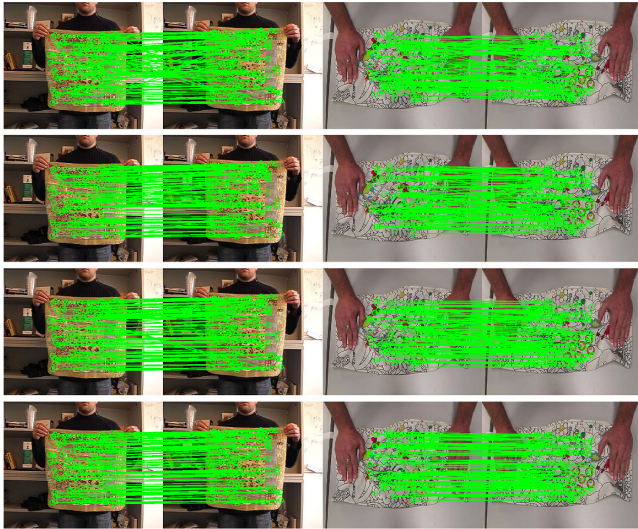

Figure 8: *Matching results. Left: cloth set, selected from frame 85 to 110, right: cushion set, selected from frames 144 to 213. Top to bottom, spectral method [Cour et al. 2006], hyper graph matching method [Zass and Shashua 2008], a Third-order tensor [Duchenne et al. 2009], and SuperMatching algorithm.*

Table 1: *Accurate rate of deformable surface matching.*

Dataset	cloth				cushion				Feature Tuples	Time (s)
Matching frames	F80-F90	F90-F95	F95-F100	F100-F105	F144-F156	F156-F165	F165-F172	F172-F188		
SuperMatching	83%	85%	84%	81%	66%	60%	69%	56%	30k	8
[Zass and Shashua 2008]	73%	79%	70%	72%	44%	39%	54%	43%	40k	6.5
[Duchenne et al. 2009]	67%	77%	73%	65%	39%	31%	47%	42%	1010k	13
[Cour et al. 2006]	27%	29%	22%	27%	14%	5%	28%	7%	–	5

6 Conclusion

This paper has given a novel matching algorithm named Super-Matching, which tackles the classic Computer Graphics and Computer Vision problem of matching various features for cases without any assumptions. SuperMatching is an efficient higher-order matching algorithm based on the supersymmetric affinity tensor. Our main contributions are as follows. First, we use a higher-order supersymmetric affinity tensor with a compact form to express higher-order consistency constraints of features. Secondly, we derive an efficient higher-order power iteration method, which makes significant efficiency by taking advantage of supersymmetry. Finally, we also give an efficient sampling strategy for choosing feature tuples to create the affinity tensor. It is one general matching due to independent of feature descriptors definition. The experiments on both synthetic and real 2D/3D data sets show that Super-Matching is one accurate feature matching algorithm resulting from supersymmetric geometric constraints linking feature points, whilst having competitive performance.

References

AIGER, D., MITRA, N. J., AND COHEN-OR, D. 2008. 4-points congruent sets for robust pairwise surface registration. *ACM Transactions on Graphics 27*, 3.

BERG, A. C., BERG, T. L., AND MALIK, J. 2005. Shape matching and object recognition using low distortion correspondence. In *IEEE CVPR*, 26–33.

BOKELOH, M., BERNER, A., WAND, M., SEIDEL, H.-P., AND SCHILLING, A., 2008. Slippage features. Technical Report, WSI-2008-03, University of Tübingen,.

BRONSTEIN, A. M., BRONSTEIN, M. M., GUIBAS, L. J., AND OVSJANIKOV, M. 2011. Shape google: Geometric words and expressions for invariant shape retrieval. *ACM Transactions on Graphics 30*, 1:1–1:20.

BROWN, B. J., AND RUSINKIEWICZ, S. 2007. Global non-rigid alignment of 3-d scans. *ACM Transactions on Graphics 26*.

CHANG, W., AND ZWICKER, M. 2009. Range scan registration using reduced deformable models. *Computer Graphics Forum 28*, 2, 447–456.

CHANG, W., AND ZWICKER, M. 2011. Global registration of dynamic range scans for articulated model reconstruction. *ACM Transactions on Graphics 30*, 26:1–26:15.

CHERTOK, M., AND KELLER, Y. 2010. Efficient high order matching. *IEEE Transactions on Pattern Analysis and Machine Intelligence 32*, 2205–2215.

COMANICIU, D., AND MEER, P. 2002. Mean shift: A robust approach toward feature space analysis. *IEEE Transactions on Pattern Analysis and Machine Intelligence 24*, 603–619.

CONTE, D., FOGGIA, P., SANSONE, C., AND VENTO, M. 2004. Thirty years of graph matching in pattern recognition. *International Journal of Pattern Recognition and Artificial Intelligence 18*, 3, 265–298.

COUR, T., SRINIVASAN, P., AND SHI, J. 2006. Balanced graph matching. In *NIPS*, 313–320.

DUCHENNE, O., BACH, F., KWEON, I., AND PONCE, J. 2009. A tensor-based algorithm for high-order graph matching. In *IEEE CVPR*, 1980–1987.

GELFAND, N., MITRA, N. J., GUIBAS, L. J., AND POTTMANN, H. 2005. Robust global registration. In *Symposium on Geometry processing*.

HUTTENLOCHER, D. P., AND ULLMAN, S. 1990. Recognizing solid objects by alignment with an image. *International Journal of Computer Vision 5* (November), 195–212.

JOHNSON, A. E., AND HEBERT, M. 1999. Using spin images for efficient object recognition in cluttered 3d scenes. *IEEE Transactions on Pattern Analysis and Machine Intelligence 21*, 5, 433–449.

KIM, V. G., LIPMAN, Y., AND FUNKHOUSER, T. 2011. Blended intrinsic maps. In *SIGGRAPH*, 79:1–79:12.

KINECT, 2012. Kinect homepage. http://www.xbox.com/en-US/kinect.

KOFIDIS, E., AND REGALIA, P. A. 2002. On the best rank-1 approximation of higher-order supersymmetric tensors. *SIAM Journal on Matrix Analysis and Applications 23*, 3, 863–884.

KOLDA, T. G., AND BADER, B. W. 2009. Tensor decompositions and applications. *SIAM Review 51*, 3, 455–500.

LEORDEANU, M., AND HEBERT, M. 2005. A spectral technique for correspondence problems using pairwise constraints. In *International Conference of Computer Vision*, 1482–1489.

LEUTENEGGER, S., CHLI, M., AND SIEGWART, R. 2011. Brisk: Binary robust invariant scalable keypoints. In *International Conference of Computer Vision*.

LI, H., SUMNER, R. W., AND PAULY, M. 2008. Global correspondence optimization for non-rigid registration of depth scans. *Computer Graphics Forum (Proc. SGP) 27*, 5, 1421–1430.

LIPMAN, Y., AND FUNKHOUSER, T. 2009. Möbius voting for surface correspondence. *ACM Transactions on Graphics (Proc. SIGGRAPH) 28*, 72:1–72:12.

LOWE, D. G. 2004. Distinctive image features from scale-invariant keypoints. *International Journal of Computer Vision 60*, 2, 91–110.

OVSJANIKOV, M., MRIGOT, Q., MMOLI, F., AND GUIBAS, L. 2010. One point isometric matching with the heat kernel. *Computer Graphics Forum (Proc. SGP) 29*, 5, 1555–1564.

PEKELNY, Y., AND GOTSMAN, C. 2008. Articulated object reconstruction and markerless motion capture from depth video. *Computer Graphics Forum (Proc. EuroGraphics) 27*, 2, 399–408.

PEYRÉ, G., PÉCHAUD, M., KERIVEN, R., AND COHEN, L. D. 2010. Geodesic methods in computer vision and graphics. *Foundations and Trends in Computer Graphics and Vision 5*, 197–397.

SAHILLIOGLU, Y., AND YEMEZ, Y. 2011. Coarse-to-fine combinatorial matching for dense isometric shape correspondence. *Computer Graphics Forum (Proc. SGP) 30*, 5, 1461–1470.

SUN, J., OVSJANIKOV, M., AND GUIBAS, L. 2009. A concise and provably informative multi-scale signature based on heat diffusion. In *Symposium on Geometry Processing*, 1383–1392.

SUN, J., CHEN, X., AND FUNKHOUSER, T. A. 2010. Fuzzy geodesics and consistent sparse correspondences for deformable shapes. *Computer Graphics Forum 29*, 5, 1535–1544.

TEVS, A., BOKELOH, M., WAND, M., SCHILLING, A., AND SEIDEL, H.-P. 2009. Isometric registration of ambiguous and partial data. In *IEEE CVPR*, 1185–1192.

TEVS, A., BERNER, A., WAND, M., IHRKE, I., AND SEIDEL, H.-P. 2011. Intrinsic shape matching by planned landmark sampling. *Computer Graphics Forum 30*, 2, 543–552.

TOLER-FRANKLIN, C., BROWN, B., WEYRICH, T., FUNKHOUSER, T., AND RUSINKIEWICZ, S. 2010. Multifeature matching of fresco fragments. *ACM Transactions on Graphics (Proc. SIGGRAPH ASIA) 29*, 185:1–185:12.

TORRESANI, L., KOLMOGOROV, V., AND ROTHER, C. 2008. Feature Correspondence Via Graph Matching: Models and Global Optimization. In *the 10th European Conference on Computer Vision*, Springer-Verlag, 596–609.

VAN KAICK, O., ZHANG, H., HAMARNEH, G., AND COHEN-OR, D. 2011. A survey on shape correspondence. *Computer Graphics Forum 30*, 6, 1681–1707.

WAND, M., ADAMS, B., OVSJANIKOV, M., BERNER, A., BOKELOH, M., JENKE, P., GUIBAS, L., SEIDEL, H.-P., AND SCHILLING, A. 2009. Efficient reconstruction of nonrigid shape and motion from real-time 3d scanner data. *ACM Transactions on Graphics 28*, 15:1–15:15.

WANG, A., LI, S., AND ZENG, L. 2010. Multiple order graph matching. In *IEEE ACCV*, 471–482.

WINDHEUSER, T., SCHLICKWEI, U., SCHIMDT, F. R., AND CREMERS, D. 2011. Large-scale integer linear programming for orientation preserving 3d shape matching. *Computer Graphics Forum (Proc. SGP) 30*, 5, 1471–1480.

ZASS, R., AND SHASHUA, A. 2008. Probabilistic graph and hypergraph matching. In *IEEE CVPR*, 1–8.

ZENG, Y., WANG, C., WANG, Y., GU, X., SAMARAS, D., AND PARAGIOS, N. 2010. Dense non-rigid surface registration using high-order graph matching. In *IEEE CVPR*, 382–389.